

U.S. DEPARTMENT OF COMMERCE  
NATIONAL OCEANIC AND ATMOSPHERIC ADMINISTRATION  
NATIONAL OCEAN SERVICE

## Data Acquisition & Processing Report

*Type of Survey:*        External Source Data

*Project No:*            OSD-RSD-16

*Time Frame:*          Nov 2013 - Jul 2014

### LOCALITY

*State:*                  New York

*General Locality:*    New York Coastline

**2014**

NOAA National Geodetic Survey  
Remote Sensing Division

### LIBRARY & ARCHIVES

**DATE:**

National Geodetic Survey

*Remote Sensing Division*

# Topobathy Lidar Survey Report:

***RSD Project: NY-1409 Coney Island to Montauk, NY***

***OCS Project Number: OSD-RSD-16***

***Survey Number: W00303***

February 12, 2015



## Contents

1.0	Area Surveyed .....	3
2.0	Survey Purpose .....	5
3.0	Intended Use of Survey .....	5
4.0	Data Acquisition and Processing .....	5
4.1.	Equipment.....	5
4.1.1.	Data Acquisition Hardware and Software.....	6
4.1.2.	Processing Software.....	18
4.2.	Quality Control.....	19
4.2.1.	Survey Methods & Procedures .....	19
4.3.	Data Processing Methods & Procedures .....	31
4.3.1.	Field Processing.....	31
4.3.2.	Workflow Overview .....	32
4.3.3.	Trajectory Processing.....	33
4.3.4.	Lidar Processing .....	34
4.3.5.	Lidar Editing .....	37
4.3.6.	Product Creation .....	37
4.3.7.	Imagery Processing .....	38
4.3.8.	Additional Quality Checks .....	39
4.4.	Corrections to measurements .....	39
4.4.1.	System Offsets and Lidar Calibrations .....	39
4.4.2.	Motion Corrections.....	39
4.4.3.	Environmental Parameters/Processing Settings.....	40
4.4.4.	Vertical Datum Conversions.....	40
5.0	Uncertainty .....	41
6.0	Vertical and Horizontal Control .....	44
7.0	Results and Recommendations.....	44

## 1.0 Area Surveyed

The Remote Sensing Division (RSD) under the National Geodetic Survey acquired topographic and bathymetric (topobathy) lidar and imagery data along the east coast from South Carolina to New York in accordance with the Scope of Work (SOW) for Shoreline Mapping in support of Public Law No: 113-002, Disaster Relief Appropriations Act 2013 (included in this RSD delivery package). While the SOW did not require the contractors to follow the Hydrographic Surveys Specification and Deliverables (HSSD), RSD worked with the Hydrographic Surveys Division and align with the HSSD where possible.

This survey W00300 (NC1408) is one of four regions of the Supplemental Sandy project (SSP) area which in its entirety covers 2,775 square miles along the Atlantic Coast from New York to South Carolina. All of the SSP the data was acquired and processed in 140 blocks with 6,852 1400 m x 1400 m ortho tiles and 41,388 500 m x 500 m lidar tiles. The SSP was acquired within the time range November, 2013 thru July, 2014 and the block delineation is shown in Figure 1.

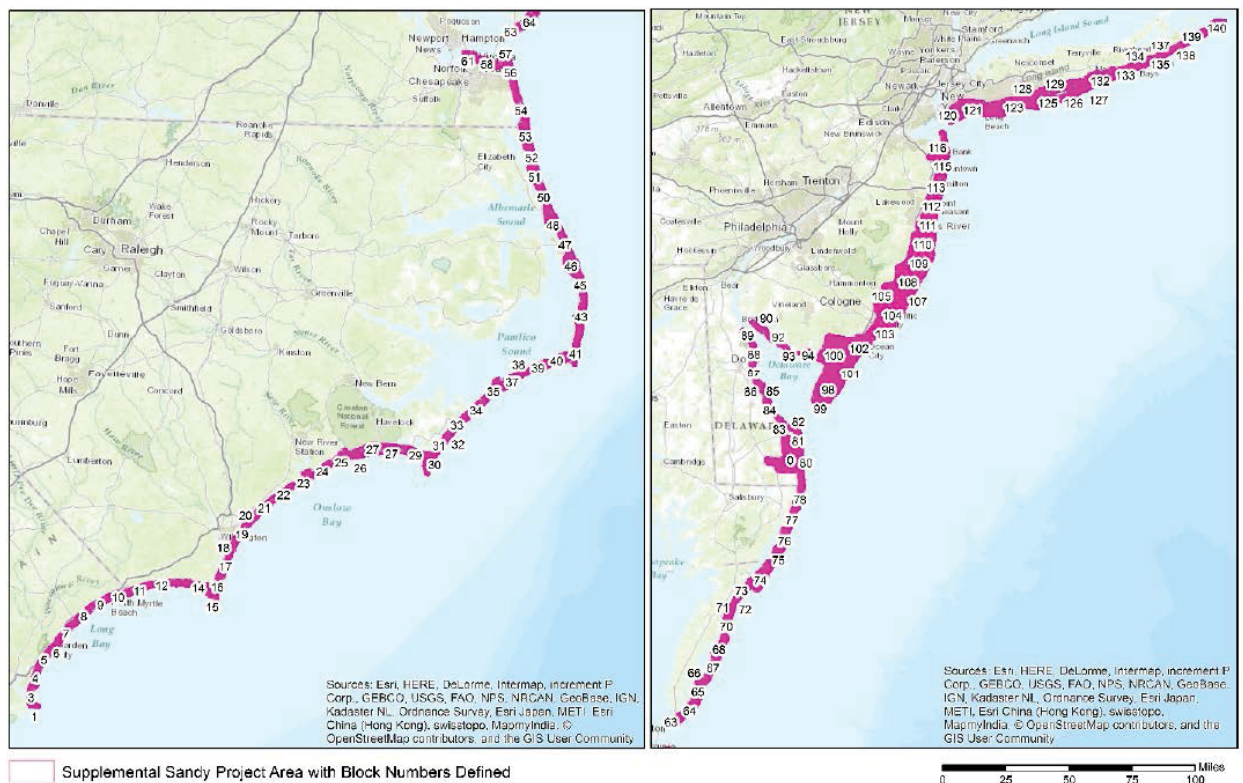


Figure 1. Supplemental Sandy Project area

Survey W00303 (NY1409) is shown in blue in Figure 2. Survey W00303 extends from Coney Island to Montauk, NY, covers blocks 119-140 and has the following survey limits listed in Table 1:

Table 1. Survey Limits for Survey W00303 (NY1409)

Northeast	Southwest
41° 05' 26.11" N	40° 31' 09.31" N
71° 49' 23.16" W	74° 03' 42.04" W

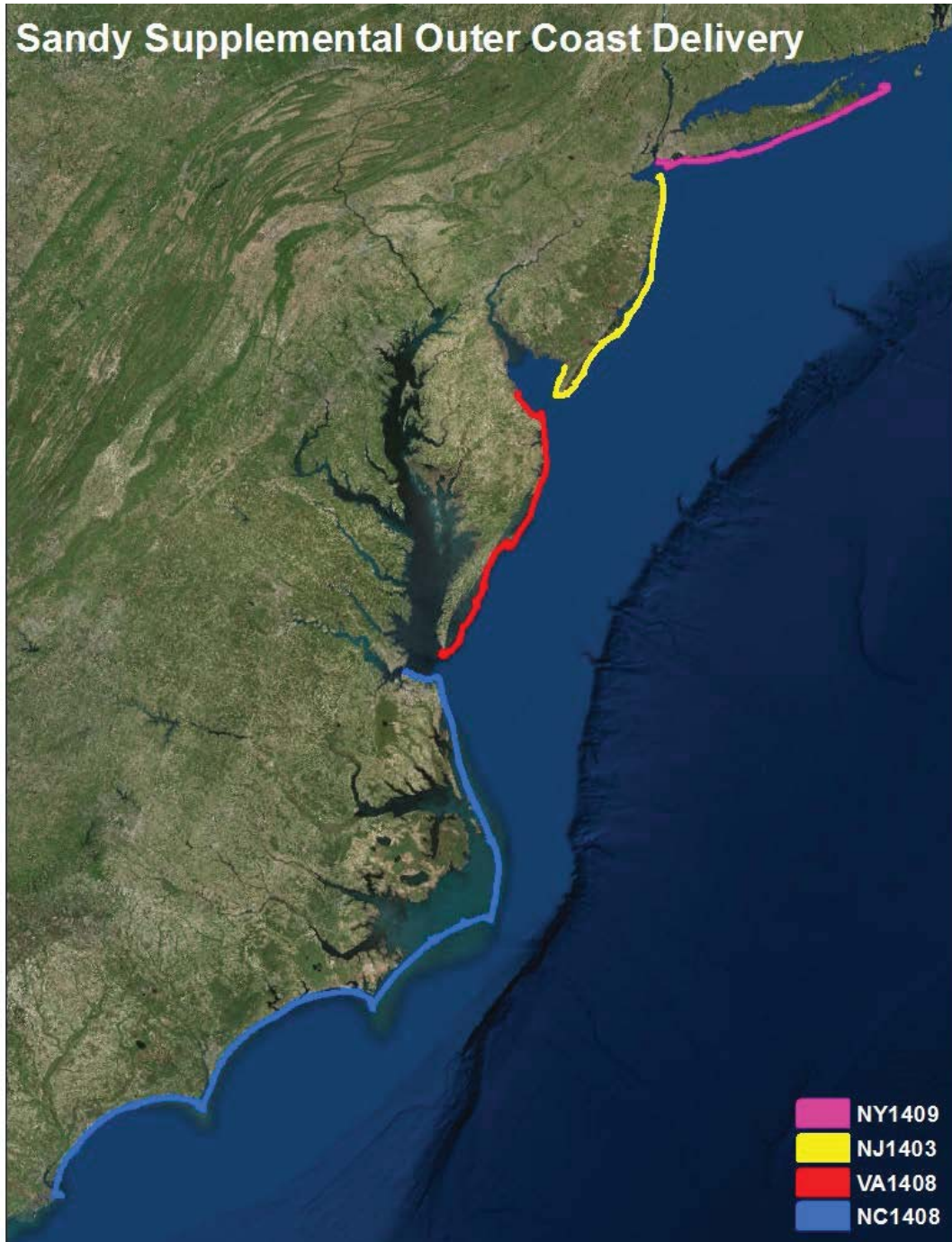


Figure 2. Supplemental Sandy project area divided into four regions for decimation to Coast Survey

## 2.0 Survey Purpose

The topo-bathy lidar and imagery data was collected through the Disaster Relief Appropriations Act 2013 following the Tropical Cyclone/Hurricane Sandy to support RSD's Coastal Mapping Program as well additional mapping and charting needs.

## 3.0 Intended Use of Survey

The survey will be used to update the shoreline and near shore bathymetric areas along the survey limits mentioned in section 1.0.

## 4.0 Data Acquisition and Processing

Dewberry served as prime contractor for the SSP. Dewberry subcontracted with Quantum Spatial (QS), Richard Crouse & Associates (RC&A), and Woolpert for various tasks on this project.

The main tasks performed by Dewberry and each sub-contractor are outlined below.

QS acquired the topobathy lidar data, calibrated all lidar data, and created the initial lidar coverages used to determine if sufficient bathymetric data had been acquired or if additional reflights were necessary.

Both Dewberry and QS processed the topobathy lidar data, including breakline collection, applying refraction corrections, and editing. Dewberry processed blocks 1-21, 63-102, 119-140, and the additional Delaware area. QS processed blocks 22-62 and 103-118.

QS acquired and processed the digital imagery for blocks 1-108 and the Delaware area. RC&A acquired the digital imagery for blocks 109-140 and Woolpert processed the digital imagery for these blocks. QS performed all ground control survey for all 140 blocks for aerotriangulation and the digital imagery processing.

The survey consisted of a minimum of  $\geq 50\%$  sidelap topobathy coverage ( $\geq 100\%$  overlap). No Automated Wreck and Obstruction Information System (AWOIS) items were required for this project.

### 4.1. Equipment

The topobathy lidar was acquired using three Riegl VG820G lidar sensors in a Cessna Caravan. The Riegl sensor was dually mounted with an accompanying NIR lidar sensor. Operational systems used to acquire survey data are described in detail in this section and listed in Table 2.

Table 2. SSP Hardware

Instrument	Manufacturer	Model	Serial No.	Function
Riegl VQ-820G (520 kHz) Topographic and Bathymetric Lidar system				
Topobathy VQ-820G which includes:	Riegl	820G	9999609, 2220530, 2220409	Topographic and Bathymetric Lidar system (532nm laser)
	Applanix POS	Version 6.2 Pack 2	N/A	Positioning and Inertial Reference System for Position, heading, roll and pitch
	Leica Leica Applanix	RCD069 RCD024 DSS 439	N/A	Digital RGB Camera
IR lidar	Riegl	420	64	Water surface detection
IR lidar	Leica	AL50	93, 94	Water surface detection
Ground Control/Ground Truth				
GNSS Receiver	Trimble	R7	N/A	Static, Rover
GNSS Receiver	Trimble	R8 Model 2	N/A	Static, Rover
GNSS Receiver	Trimble	R8 Model 3	N/A	Static, Rover
GNSS Receiver	Leica	GS-15	N/A	Static, Rover

#### 4.1.1. Data Acquisition Hardware and Software

##### 4.1.1.1. Aircraft

QSI operated a single engine Cessna Caravan N704MD (Figure 3) as the survey aircraft for the SSP. Airborne collection logs and situation reports provided to NOAA throughout the acquisition process were in the form of a daily Sitrep. These Sitreps have been compiled into three PDFs (e.g. Situation Report NOAA Sandy Restoration Shoreline Mapping C1 Bocks 119 through 140) and reports the collection date, tide window, lines collected and operators notes.



*Figure 3. QSI's Cessna Caravan used for SSP*

#### 4.1.1.2. lidar system

The Cessna Caravan was equipped with a Riegl VQ-820G topographic and bathymetric lidar system (Figure 3) for the SSP from November 21, 2013 – Jul 27, 2014. The Riegl 820G acquires bathymetric lidar, topographic lidar and digital imagery simultaneously. The bathymetric and topographic lasers are independent and do not share an optical chain or receivers; each system is optimized for the role it performs. The Riegl 820G bathymetric laser operates in the green spectrum at 532nm, has an effective measurement rate of 200,000 measurements per second and is designed to penetrate to approximately 1 secchi depth depending on water clarity and seafloor reflectivity. Additionally, the Riegl 820G has an arc-like scan pattern on the ground/seafloor.

The bathymetric laser settings are listed in Table 3.



Table 3. Bathymetric lidar specifications and settings

<b>Bathymetric LiDAR Survey Settings &amp; Specifications</b>		
<b>Flight Plan</b>	300 meter AGL	600 meter AGL
<b>Aircraft Used</b>	Cessna Caravan	Cessna Caravan
<b>Sensors</b>	Riegl VQ-820G	Riegl-VQ-820G
<b>Survey Altitude (AGL)</b>	300 m	600 m
<b>Target Pulse Rate</b>	284 kHz	284 kHz
<b>Pulse Mode</b>	Single Pulse in Air (SPiA)	Single Pulse in Air (SPiA)
<b>Laser Pulse Diameter</b>	30 cm	60 cm
<b>Planned Swath</b>	218 m	437 m
<b>Speed:</b>	110 knots	110 knots
<b>Field of View</b>	40°	40°
<b>GPS Baselines</b>	≤13 NM	≤13 NM
<b>GPS PDOP</b>	≤3.0	≤3.0
<b>GPS Satellite Constellation</b>	≥6	≥6
<b>Maximum Returns</b>	4	4
<b>Intensity</b>	8-bit	8-bit
<b>Resolution/Density</b>	≥4 pulses/m <sup>2</sup>	≥4 pulses/m <sup>2</sup>
<b>Accuracy</b>	RMSE <sub>z</sub> ≤ 12.5 cm land RMSE <sub>z</sub> ≤ 25 cm submerged land	RMSE <sub>z</sub> ≤ 12.5 cm land RMSE <sub>z</sub> ≤ 25 cm submerged land

QSI utilized two different flight plans based on the survey altitude, in order to capture the best shallow-water topobathy dataset possible. Near-shore flight plans were executed at an above-ground level (AGL) of 600 meters, while flight plans over ocean waters were executed at an AGL of 300 meters. Both plans are provided in Table 4.

Table 4. NIR sensor specifications and survey settings

Near-Infrared LiDAR Survey Settings & Specifications		
Flight Plan	300 meter AGL	600 meter AGL
Aircraft Used	Cessna Caravan or 206	Cessna Caravan or 206
Sensors	Leica ALS50 or Riegl VQ-420	Leica ALS50 or Riegl VQ-420
Survey Altitude (AGL)	300 m	600 m
Target Pulse Rate	150 kHz	135 kHz
Pulse Mode	Single Pulse in Air (SPiA)	Single Pulse in Air (SPiA)
Laser Pulse Diameter	11 cm	15 cm
Planned Swath	218 m	437 m
Speed:	110 knots	110 knots
Mirror Scan Rate	45.1 Hz	45.1 Hz
Field of View	40°	40°
GPS Baselines	≤13 NM	≤13 NM
GPS PDOP	≤3.0	≤3.0
GPS Satellite Constellation	≥6	≥6
Maximum Returns	4	4
Intensity	8-bit (16-bit for Riegl)	8-bit (16-bit for Riegl)
Resolution/Density	≥4 pulses/m <sup>2</sup>	≥4 pulses/m <sup>2</sup>
Accuracy	RMSE <sub>Z</sub> ≤ 12.5 cm land	RMSE <sub>Z</sub> ≤ 12.5 cm land

Additional flight details regarding the each flight plan (for 300m or 600m plan) can be found in the SSP report submitted by NGS' contractors.

GPS data was recorded at 2Hz and the IMU data was recorded 200Hz.

4.1.1.3. GNSS ground control equipment

Ground control surveys, including monumentation, aerial targets and ground survey points (GSPs), were conducted to support the airborne acquisition. Ground control data were used to geospatially correct the aircraft positional coordinate data and to perform quality assurance checks on final LiDAR data.

**Monumentation**

The spatial configuration of ground survey monuments provided redundant control within 13 nautical miles of the mission areas for LiDAR flights. Monuments were also used for collection of ground survey points using real time kinematic (RTK), post processed kinematic (PPK), and fast-static (FS) survey techniques. Monument locations were selected with consideration for satellite visibility, field crew safety, and optimal location for GSP coverage. QSI utilized 68 existing NGS monuments, one existing US Coast Guard tidal station, 21 existing active Continuously Operating Reference Stations (CORS), and 54 newly established monuments for the LiDAR project (Table 5). New monumentation was set using 5/8" x 30" rebar topped with stamped 2" aluminum caps. Active CORS were utilized from the NGS, KeyNet, North Carolina RTN, and South Carolina CORS networks. QSI's team of professional land surveyors oversaw all ground survey work.

National Geodetic Survey

Remote Sensing Division

Table 5. Monuments established for the NOAA Sandy Shoreline Mapping acquisition. Coordinates are on the NAD83 (2011) datum, epoch 2010.00

Monument ID	Origin	Latitude	Longitude	Ellipsoid (meters)
AA5233	NGS	40° 09' 09.59979"	-74° 04' 12.87493"	-12.038
AA7211	NGS	39° 17' 45.31227"	-75° 10' 19.93126"	-31.232
AA7217	NGS	39° 17' 29.68858"	-75° 11' 50.27041"	-33.214
AA9307	NGS	39° 11' 57.18157"	-75° 29' 13.14069"	-28.003
AB6715	NGS	38° 57' 19.59768"	-74° 52' 19.98063"	-33.482
AB6826	NGS	33° 54' 21.43907"	-78° 26' 24.10831"	-25.890
AE8345	NGS	33° 43' 04.43334"	-78° 53' 10.25021"	-28.111
AF8821	NGS	35° 13' 08.76078"	-75° 41' 38.23116"	-38.035
AI9354	NGS	39° 30' 45.40675"	-74° 19' 10.82475"	-33.127
AJ4587	NGS	37° 36' 14.13270"	-75° 41' 18.27016"	-35.290
AJ7998	NGS	38° 06' 46.20539"	-75° 23' 26.92826"	-24.932
CMAP	NGS	39° 00' 20.58726"	-74° 54' 28.36186"	-24.577
DD0317	NGS	33° 18' 55.79572"	-79° 19' 21.55414"	-23.179
DEMI	NGS	38° 36' 36.97516"	-75° 12' 10.31480"	-26.102
DF5594	NGS	36° 32' 46.32422"	-76° 00' 04.08751"	-36.333
DF5617	NGS	36° 15' 57.54984"	-75° 47' 24.04012"	-36.948
DG9068	NGS	36° 51' 19.67137"	-76° 18' 04.66904"	-34.637
DH7883	NGS	38° 09' 03.57467"	-75° 17' 24.48168"	-32.490
DH7884	NGS	38° 09' 00.69040"	-75° 17' 19.70022"	-32.996
DI0949	NGS	38° 46' 52.74795"	-75° 06' 37.17731"	-34.483
DI0955	NGS	38° 27' 50.93456"	-75° 09' 56.36484"	-29.618
DI0957	NGS	38° 37' 31.33613"	-75° 06' 02.79722"	-34.744
DK3488	NGS	35° 10' 50.88304"	-75° 47' 02.13165"	-37.305

Monument ID	Origin	Latitude	Longitude	Ellipsoid (meters)
DK3492	NGS	35° 53' 05.30811"	-75° 35' 21.24786"	-37.862
DK3494	NGS	35° 15' 06.46066"	-75° 31' 34.42819"	-36.135
DL3262	NGS	33° 33' 18.24453"	-79° 12' 59.65298"	-28.213
DL3270	NGS	33° 29' 10.29033"	-79° 05' 40.90653"	-31.587
DL3311	NGS	33° 49' 55.48316"	-78° 40' 10.31884"	-26.972
DM3311	NGS	33° 15' 04.94266"	-79° 16' 12.43653"	-33.576
DM5989	NGS	39° 57' 13.90068"	-74° 09' 43.57246"	-22.362
DN6296	NGS	35° 26' 19.46877"	-75° 29' 09.20737"	-37.399
DN6303	NGS	35° 36' 54.87396"	-75° 28' 06.04639"	-37.743
DN8307	NGS	39° 24' 45.56553"	-74° 29' 29.95957"	-32.567
DN8361	NGS	39° 18' 01.78391"	-75° 30' 16.03394"	-30.205
DN8362	NGS	39° 15' 33.52247"	-75° 28' 23.06844"	-31.519
DN9213	NGS	38° 49' 47.33431"	-75° 14' 57.89224"	-34.267
EA0275	NGS	34° 41' 04.39965"	-76° 31' 36.23673"	-36.952
EVS4	CORS	36° 49' 25.83091"	-76° 03' 14.55324"	-26.362
EX0206	NGS	35° 39' 41.10224"	-75° 28' 44.21625"	-35.770
EX0216	NGS	35° 31' 53.79816"	-75° 28' 21.90261"	-37.403
EX0274	NGS	35° 08' 31.60095"	-75° 53' 20.09205"	-34.966
EX0689	NGS	35° 06' 13.51127"	-75° 57' 44.52960"	-37.086
FE01	CORS	39° 26' 32.64943"	-75° 16' 00.98553"	-0.338

## National Geodetic Survey

*Remote Sensing Division*

Monument ID	Origin	Latitude	Longitude	Ellipsoid (meters)
FW0050	NGS	36° 06' 00.20307"	-75° 42' 57.62465"	-29.603
FW0072	NGS	36° 00' 05.86666"	-75° 39' 14.49357"	-36.198
FW0217	NGS	37° 24' 39.73316"	-75° 53' 57.21139"	-26.253
FW0685	NGS	36° 10' 51.79417"	-75° 45' 22.30565"	-36.588
FX2972	NGS	36° 47' 47.95547"	-76° 01' 19.14077"	-32.750
HU0176	NGS	38° 56' 08.49307"	-75° 19' 04.82459"	-33.610
HU0197	NGS	38° 48' 46.81442"	-75° 15' 10.80872"	-33.777
HU1256	NGS	38° 23' 10.70353"	-75° 04' 27.89352"	-33.038
HU1350	NGS	38° 47' 10.09242"	-75° 09' 29.81712"	-30.762
HU1583	NGS	38° 11' 57.30643"	-75° 09' 21.86138"	-34.810
JU0159	NGS	39° 42' 07.13824"	-74° 08' 10.53617"	-32.016
JU0235	NGS	39° 32' 07.60906"	-74° 19' 21.17006"	-33.177
JU0415	NGS	39° 06' 32.97042"	-74° 47' 47.37808"	-31.352
JU2304	NGS	39° 14' 06.09667"	-74° 57' 56.10313"	-30.561
JU2416	NGS	39° 18' 26.45499"	-74° 37' 08.13719"	-29.727
JU4135	NGS	39° 06' 40.25959"	-75° 27' 45.93340"	-30.529
JU4429	NGS	39° 10' 53.01734"	-74° 43' 25.41134"	-31.334
JU4439	NGS	39° 30' 34.37075"	-74° 31' 11.83716"	-19.192
JU4443	NGS	39° 00' 11.70224"	-74° 52' 13.38458"	-34.456
JU4458	NGS	39° 13' 57.23936"	-74° 40' 20.27352"	-33.280
KU1383	NGS	40° 35' 03.58752"	-73° 52' 50.32518"	-29.271
KU3380	NGS	40° 34' 18.30610"	-73° 52' 15.43569"	-29.119
KU4164	NGS	40° 56' 13.69266"	-72° 12' 52.35763"	-28.363
KU4974	NGS	40° 35' 39.97030"	-73° 31' 36.61081"	-28.034
KV6783	NGS	40° 01' 04.01439"	-74° 04' 55.99004"	-32.034
KV7023	NGS	40° 03' 18.02744"	-74° 08' 36.50272"	-25.506
LOY2	CORS	36° 45' 50.43174"	-76° 14' 16.06799"	-23.439
LOYW	CORS	37° 31' 40.99508"	-75° 50' 52.66270"	-22.486
LS03	CORS	36° 47' 19.43630"	-75° 57' 34.32996"	-22.006
LX5588	NGS	41° 00' 50.22485"	-72° 00' 22.36880"	9.869

Monument ID	Origin	Latitude	Longitude	Ellipsoid (meters)
NCBE	CORS	34° 43' 08.50895"	76° 40' 18.99140"	-27.858
NCBI	CORS	35° 50' 44.35730"	-75° 33' 48.94199"	-33.046
NCBX	CORS	35° 15' 58.08197"	-75° 33' 06.82885"	-25.445
NCCI	CORS	35° 01' 03.76013"	-76° 18' 55.28490"	-30.613
NCDU	CORS	36° 10' 54.01098"	-75° 45' 04.79522"	-24.775
NCEL	CORS	36° 20' 28.79075"	-76° 15' 29.27386"	-29.750
NCFF	CORS	33° 57' 38.26113"	-77° 56' 18.76581"	-29.165
NCSL	CORS	33° 58' 57.20129"	-78° 23' 24.30664"	-10.002
NJBR	CORS	39° 25' 24.24019"	-75° 12' 25.41542"	-0.223
NJCM	CORS	39° 06' 02.39693"	-74° 48' 10.42433"	-25.313
NJGT	CORS	39° 28' 28.25439"	-74° 31' 50.93862"	-11.096
NJOC	CORS	39° 57' 10.02328"	-74° 11' 36.59328"	-8.184
NOAA_SANDY_001	QSI	37° 46' 28.62869"	-75° 33' 41.11517"	-35.355
NOAA_SANDY_002	QSI	37° 44' 05.61661"	-75° 36' 08.19652"	-32.344
NOAA_SANDY_003	QSI	37° 45' 44.49651"	-75° 40' 02.52660"	-24.975
NOAA_SANDY_004	QSI	37° 33' 34.04574"	-75° 49' 03.02355"	-26.152
NOAA_SANDY_005	QSI	37° 23' 36.80297"	-75° 53' 15.07155"	-27.622
NOAA_SANDY_006	QSI	39° 12' 13.30469"	-74° 53' 28.80029"	-32.522
NOAA_SANDY_007	QSI	37° 52' 54.88819"	-75° 29' 29.68422"	-35.443
NOAA_SANDY_008	QSI	37° 55' 18.94608"	-75° 21' 09.82198"	-35.863
NOAA_SANDY_009	QSI	37° 08' 41.37652"	-75° 57' 47.07743"	-31.341
NOAA_SANDY_010	QSI	37° 17' 08.05663"	-75° 55' 30.29255"	-34.979
NOAA_SANDY_011	QSI	37° 13' 30.08375"	-75° 58' 14.41731"	-26.684
NOAA_SANDY_013	QSI	39° 08' 58.55845"	-75° 26' 39.23014"	-32.538
NOAA_SANDY_100	QSI	40° 47' 01.84683"	-72° 47' 07.70296"	-30.634
NOAA_SANDY_101	QSI	40° 49' 21.68560"	-72° 37' 08.19723"	-29.122
NOAA_SANDY_102	QSI	40° 42' 41.50512"	-73° 14' 36.51200"	-29.834
NOAA_SANDY_103	QSI	40° 38' 16.87965"	-73° 19' 49.66518"	-27.602
NOAA_SANDY_104	QSI	40° 46' 26.30691"	-72° 53' 47.55108"	-30.717
NOAA_SANDY_105	QSI	40° 37' 15.57395"	-73° 37' 36.93448"	-29.881

## National Geodetic Survey

*Remote Sensing Division*

Monument ID	Origin	Latitude	Longitude	Ellipsoid (meters)
NOAA_SANDY_106	QSI	40° 37' 15.61071"	-73° 37' 35.75537"	-29.595
NOAA_SANDY_107	QSI	40° 35' 00.70970"	-73° 52' 51.78925"	-28.881
NOAA_SANDY_108	QSI	40° 34' 02.88023"	-73° 52' 12.24056"	-29.281
NOAA_SANDY_133	QSI	39° 51' 21.96133"	-74° 07' 58.75769"	-31.594
NOAA_SANDY_135	QSI	40° 16' 35.84477"	-74° 02' 35.90240"	-17.318
NOAA_SANDY_137	QSI	40° 23' 40.45612"	-73° 58' 37.35725"	-28.938
NOAA_SANDY_139	QSI	40° 21' 46.76782"	-74° 02' 25.39457"	-27.111
NOAA_SANDY_201	QSI	36° 53' 05.36583"	-76° 11' 54.53373"	-31.481
NOAA_SANDY_201A	QSI	34° 24' 14.21760"	-77° 37' 26.62162"	-29.211
NOAA_SANDY_202	QSI	34° 28' 52.82128"	-77° 30' 30.54214"	-28.288
NOAA_SANDY_203	QSI	36° 54' 24.71369"	-76° 05' 36.09365"	-34.658
NOAA_SANDY_204	QSI	34° 38' 55.31184"	-77° 12' 42.91167"	-27.688
NOAA_SANDY_205	QSI	36° 49' 23.17242"	-75° 58' 49.15912"	-35.514
NOAA_SANDY_206	QSI	34° 12' 44.82265"	-77° 49' 07.73206"	-35.813
NOAA_SANDY_207	QSI	36° 23' 20.82838"	-75° 49' 51.18852"	-36.564
NOAA_SANDY_207_RESET	QSI	36° 23' 16.66692"	-75° 49' 50.11483"	-35.790
NOAA_SANDY_208	QSI	34° 06' 26.64414"	-77° 55' 18.77366"	-35.879
NOAA_SANDY_210	QSI	33° 57' 35.39293"	-77° 56' 23.60443"	-36.435
NOAA_SANDY_212	QSI	33° 56' 18.19023"	-78° 03' 56.90515"	-31.859
NOAA_SANDY_214	QSI	33° 54' 53.71905"	-78° 15' 22.19165"	-34.103
NOAA_SANDY_215	QSI	33° 33' 04.25648"	-79° 02' 29.82388"	-32.391
NOAA_SANDY_216	QSI	33° 22' 40.14761"	-79° 09' 19.29367"	-32.665
NOAA_SANDY_217	QSI	33° 34' 14.00936"	-79° 01' 54.00099"	-28.042
NOAA_SANDY_219	QSI	33° 42' 56.44408"	-78° 53' 12.01254"	-28.076
NOAA_SANDY_220	QSI	36° 32' 05.45273"	-75° 55' 32.74863"	-34.117
NOAA_SANDY_221	QSI	33° 25' 29.10785"	-79° 07' 44.25932"	-33.298
NOAA_SANDY_223	QSI	34° 40' 31.68954"	-76° 57' 25.25685"	-31.929
NOAA_SANDY_225	QSI	34° 41' 54.58257"	-76° 46' 58.87452"	-35.068
NOAA_SANDY_227	QSI	34° 41' 04.18252"	-76° 31' 41.55247"	-36.706
NOAA_SANDY_229	QSI	34° 53' 44.24886"	-76° 19' 25.29923"	-36.754



Monument ID	Origin	Latitude	Longitude	Ellipsoid (meters)
NOAA_SANDY_231	QSI	40° 53' 10.29158"	-72° 30' 05.99342"	-30.230
NOAA_SANDY_232	QSI	40° 53' 36.19817"	-72° 20' 37.25972"	-30.149
NOAA_SANDY_233	QSI	40° 44' 49.43234"	-73° 01' 38.07902"	-30.494
NOAA_SANDY_243	QSI	36° 54' 24.84487"	-76° 05' 36.64422"	-34.756
NOAA_SANDY_244	QSI	36° 57' 29.63040"	-76° 15' 33.34215"	-34.262
OCS_NJ_03	QSI	39° 39' 04.49093"	-74° 11' 06.98918"	-32.653
SCHG	CORS	33° 47' 47.19678"	-79° 00' 12.54582"	-10.490
SCHY	CORS	33° 56' 23.73651"	-78° 44' 06.88294"	-16.038
TIDAL	USCG	35° 47' 55.36401"	-75° 32' 50.24751"	-38.043
VAWI	CORS	37° 56' 03.49970"	-75° 28' 15.94918"	-22.324
ZNY1	CORS	40° 47' 03.54971"	-73° 05' 49.78067"	7.265

To correct the continuously recorded onboard measurements of the aircraft position, QSI concurrently conducted multiple static Global Navigation Satellite System (GNSS) ground surveys (1 Hz recording frequency) over each monument. During post-processing, the static GPS data were triangulated with nearby NGS CORS using the Online Positioning User Service (OPUS) for precise positioning. Multiple independent sessions over the same monument were processed to confirm antenna height measurements and to refine position accuracy.

Monuments were established according to the national standard for geodetic control networks, as specified in the Federal Geographic Data Committee (FGDC) Geospatial Positioning Accuracy Standards for geodetic networks. This standard provides guidelines for classification of monument quality at the 95% confidence interval as a basis for comparing the quality of one control network to another. The monument rating for this project is shown in Table 6.

Table 6. Federal Geographic Data Committee monument rating for network accuracy Federal Geographic Data Committee monument rating for network accuracy

Direction	Rating
1.96 * St Dev <sub>NE</sub> :	0.050 m
1.96 * St Dev <sub>Z</sub> :	0.050 m

For the NOAA Sandy Shoreline Mapping LiDAR project, the monument coordinates contributed no more than 7.1 cm of positional error to the geolocation of the final ground survey points and LiDAR, with 95% confidence.

**Ground Survey Points (GSPs)**

Ground survey points were collected using real time kinematic, post-processed kinematic (PPK), and/or fast-static (FS) survey techniques. A base unit was positioned at a nearby monument to broadcast a kinematic correction to a roving GNSS receiver. All GSP measurements were made during periods with a Position Dilution of Precision (PDOP) of  $\leq 3.0$  with at least six satellites in view of the stationary and roving receivers. When collecting RTK and PPK data, the rover records data while stationary for five or more seconds, then calculates the pseudorange position using at least three one-second epochs. FS surveys record observations for up to fifteen minutes on each GSP in order to support longer baselines for post-processing. Relative errors for any GSP position must be less than 1.5 cm horizontal and 2.0 cm vertical in order to be accepted. See Table 7 for receiver specifications.

GSPs were collected in areas where good satellite visibility was achieved on paved roads and other hard surfaces such as gravel or packed dirt roads. GSP measurements were not taken on highly reflective surfaces such as center line stripes or lane markings on roads due to the increased noise seen in the laser returns over these surfaces. GSPs were collected within as many flightlines as possible; however the distribution of GSPs depended on ground access constraints and monument locations and may not be equitably distributed throughout the study area.

*Table 7. Trimble equipment identification*

Receiver Model	Antenna	OPUS Antenna ID	Use
Trimble R7 GNSS	Zephyr GNSS Geodetic Model 2 RoHS	TRM57971.00	Static, Rover
Trimble R8 Model 2	Integrated Antenna	TRM_R8_GNSS	Static, Rover
Trimble R8 Model 3	Integrated Antenna	TRM_R8_GNSS3	Static, Rover
Leica GS-15	Integrated Antenna	LEIGS15	Static, Rover

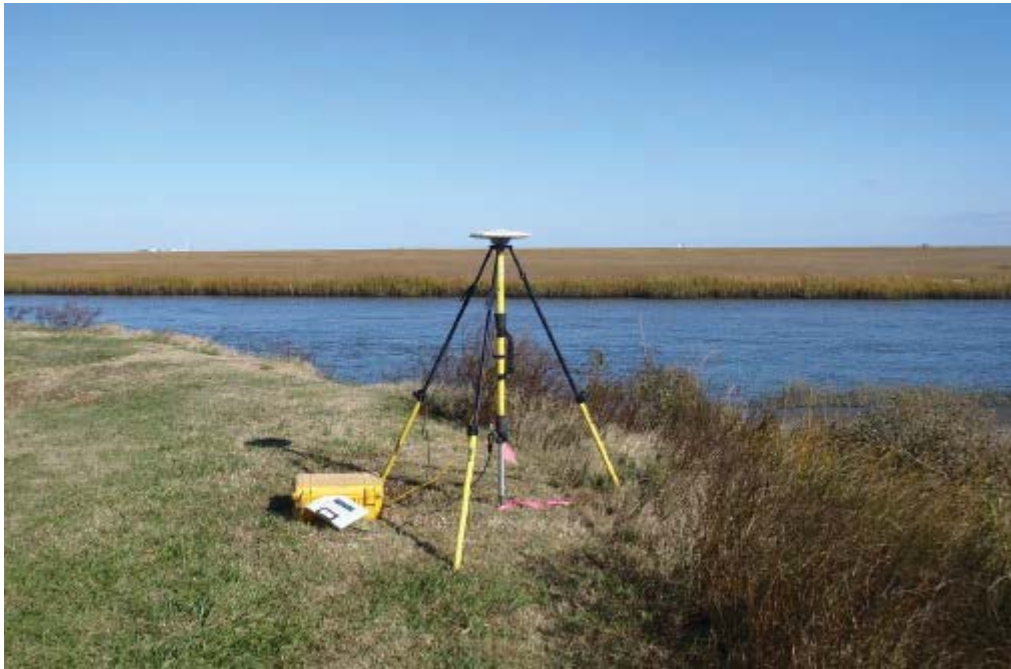


Figure 4. Photo taken by QSI acquisition staff shows a view of static GNSS Trimble equipment set up over monument NOAA\_Sandy\_001

#### 4.1.2. Processing Software

A list of the processing software used in during the SSP is provided in Table 4.

Table 8. Processing Software

Description	Manufacturer	Version	Description
RiProcess	Riegl	1.6	Laser return position computations
Terra Match	TerraSolid	14	
Global Mapper	Blue Marble Geographics	V15	to create grids and review water surface models
GeoCue	GeoCue	2014	to create DZ orthos
TerraScan	TerraSolid	14	to look at profiles of identified cultural or planar features to look for agreement or discrepancies between NIR/Green datasets
ArcGIS	ESRI	10	to convert NoData pixels to polygons
QT Modeler	Applied Imagery	7-1-4	interim QC

## 4.2. Quality Control

### 4.2.1. Survey Methods & Procedures

In preparation for data collection, QSI reviewed the project areas and developed specialized flight plans to ensure complete coverage of the LiDAR study area at the target point density of  $\geq 4.0$  points/m<sup>2</sup>. Acquisition parameters including orientation relative to terrain, flight altitude, pulse rate, scan angle, and ground speed were adapted to optimize flight paths and flight times while meeting all contract specifications.

Factors such as satellite constellation availability and weather windows were considered during the planning stage. Due to the widespread and complex acquisition, QSI reviewed several factors prior to each LiDAR mission; suitable water clarity for bathymetric data collection, restricted or controlled airspace requirements, notice-to-airman required prior to each flight, ~15km flightline lengths, and ~20% of lines at MLLW (Mean Lower Low Water levels) or optimal tide levels. Any weather hazards or conditions affecting the flights were continuously monitored due to their potential impact on the daily success of airborne and ground operations. Water clarity was carefully monitored and recorded throughout the project.

The biggest problem encountered was weather. Acquisition began in November of 2013 but was not complete until July 2014 due to numerous weather delays. QS quickly used the allotted number of stand-by days. To minimize the number of stand-by days and reduce the cost of having aircraft mobilized, QS would move the aircraft to other areas of the Sandy project where weather was better or would acquire other lidar projects when possible. But because the Sandy Area of Interest (AOI) is so large, the original intent was to finish acquisition in stages so that calibration and processing could begin on some of the data while acquisition was still being completed in other areas. Constantly moving the aircraft to accommodate weather prevented any portion of the project from being calibrated ahead of the rest of the AOI in any meaningful manner. This severely impacted the rest of the schedule and caused significant delays. Additionally, moving the aircraft to other areas before one contiguous block was fully acquired resulted in significant time differences between the acquisition of the 600 m AGL and 300 m AGL flight lines. The time difference in acquisition of these overlapping and adjacent flight lines translated into temporal differences in the submerged topography and near shore data. An additional classification, class 31-temporal bathy bottom, was added to the final classification schema to accommodate these temporal differences within the data.

#### 4.2.1.1. lidar calibration

A calibration site was selected in a suburban environment with many houses that have pitched roofs and open flat surfaces, such as cul-de-sac roads. The GPS baseline between the base station and aircraft are kept to a minimum, so that the uncertainties associated with the trajectory file are minimized. The raw data was initially processed to a point cloud referenced to an appropriate coordinate system. The initial boresight angles were calculated and verified in a three-step procedure. First, an initial examination of the relative offset between adjacent scan lines is performed. This offset observed is utilized to assist in finding tie objects between different scans. A tie object is a planar surface, point, or sphere found in a scan. Observations consist of the matching of two similar objects in overlapping scans. Between 30,000 to 70,000 observations are typically identified for a geometric calibration flight. Second, the distances of the observations and a standard deviation are calculated for estimation of the current fit. Third, an adjustment is calculated for optimal boresight angles to achieve a best fit between all scans in the data set. The data is then reprocessed with the newly calculated boresight angles. The third step was repeated until the standard deviation of distances between objects converges to a value between 1 to 3 cm and further adjustment iterations are providing negligible differences. Various techniques are utilized to analyze the results from qualitative examination of intensity data and hillshade images to examine for unusual scan or geometrical artifacts to quantitative differences between flat surfaces in overlapping scans.

#### 4.2.1.2. Survey

All survey data collection was conducted at an altitude of 300 and 600m at around 110 knots giving a nominal pulse density of 4 m<sup>2</sup> for the bathymetric laser and a ground sample distance of 35 cm for the rectified imagery mosaic for 100% coverage. The Riegl 820G simultaneously acquired topographic and bathymetric lidar at 284 kHz and digital camera imagery with an opposing flight line side-lap of ≥50% (≥100% overlap) in order to reduce laser shadowing and increase surface laser painting.

##### **Flight Details**

The following table provides a list of airborne acquisition dates for all of the SSP, as well as pertinent information including which sensor and plane were utilized. In total, QSI conducted 262 LiDAR missions. LiDAR survey settings for each flight plan (300 meter or 600 meter plan,) are provided in Table 9.

Table 9. Flight Details

Flight Date	Sensors Used	Planned AGL (meters)	Plane	Containing Block	Camera
11/21/13	S609/SN094	600	704MD	71	RCD069
11/22/13	S609/SN094	600	704MD	70, 71	RCD069
11/23/13	S609/SN094	600	704MD	69, 71	RCD069
11/24/13	S609/SN094	600	704MD	67, 68	RCD069
11/25/13	S609/SN094	600	704MD	75, 76	RCD069
11/29/13	S609/SN094	600	704MD	82, 83	RCD069
11/30/13	S609/SN094	600	704MD	84, 85, 86	RCD069
12/01/13	S609/SN094	600	704MD	87, 88	RCD069
12/02/13	S609/SN094	600	704MD	89, 90, 91	RCD069
12/03/13	S609/SN094	600	704MD	92, 93	n/a
12/11/13	S609/SN094	600	704MD	94	RCD069
12/13/13	S609/SN094	600	704MD	72	RCD069
12/15/13	S609/SN094	600	704MD	74	RCD069
12/16/13	S609/SN094	600	704MD	74	RCD069
12/17/13	S609/SN094	600	704MD	76, 77	RCD069
12/18/13	S609/SN094	600	704MD	77, 78	RCD069
12/19/13	S609/SN094	600	704MD	78, 79	RCD069
12/20/13	S609/SN094	600	704MD	73, 74	RCD069
12/21/13	S609/SN094	600	704MD	79, 80	n/a
12/28/13	S409/SN064	600	5726J	67	n/a
12/28/13	S609/SN094	600	704MD	81	RCD024
12/30/13	S409/SN064	600	5726J	65, 66	n/a
12/30/13	S609/SN094	600	704MD	100	n/a
12/31/13	S409/SN064	600	5726J	64, 65	n/a
12/31/13	S609/SN094	600	704MD	94, 95, 100	RCD024
01/01/14	S409/SN064	600	5726J	63, 64	n/a

National Geodetic Survey

*Remote Sensing Division*

Flight Date	Sensors Used	Planned AGL (meters)	Plane	Containing Block	Camera
01/01/14	S609/SN094	600	704MD	96, 97	RCD024
01/04/14	S409/SN064	600	5726J	55	n/a
01/06/14	S609/SN094	600	704MD	22	RCD024
01/07/14	S409/SN064	600	5726J	57	n/a
01/07/14	S609/SN094	600	704MD	19, 20, 21	RCD024
01/08/14	S409/SN064	600	5726J	54	n/a
01/08/14	S609/SN094	600	704MD	17, 18, 19	RCD024
01/09/14	S409/SN064	600	5726J	53	n/a
01/09/14	S609/SN094	600	704MD	16, 17	RCD024
01/12/14	S609/SN094	300	704MD	19, 20	RCD024
01/13/14	S609/SN094	300	704MD	20, 21	RCD024
01/17/14	S409/SN064	600	5726J	56	n/a
01/19/14	S409/SN064	600	5726J	56, 58	n/a
01/20/14	S409/SN064	600	5726J	50, 51	n/a
01/20/14	S609/SN094	600	704MD	13, 14	RCD024
01/21/14	S609/SN094	600	704MD	12, 13	RCD024
01/22/14	S609/SN094	600	704MD	9, 10	RCD024
01/23/14	S609/SN094	600	704MD	10	RCD024
01/23/14	S609/SN094	600	704MD	10, 11	RCD024
01/24/14	S409/SN064	600	5726J	46	n/a
01/24/14	S609/SN094	600	704MD	11, 12	n/a
01/25/14	S609/SN094	600	704MD	7, 8	RCD024
01/26/14	S409/SN064	600	5726J	43, 44	n/a
01/26/14	S609/SN094	600	704MD	6, 7	RCD024
01/27/14	S609/SN094	600	704MD	5, 6	RCD024
01/31/14	S609/SN094	600	704MD	3, 4	RCD024
02/02/14	S609/SN094	600	704MD	1, 2, 3	RCD024
02/06/14	S609/SN094	600	704MD	23, 24	n/a
02/07/14	S409/SN064	600	5726J	47	n/a
02/07/14	S609/SN094	600	704MD	24, 25, 26	n/a

National Geodetic Survey

*Remote Sensing Division*

Flight Date	Sensors Used	Planned AGL (meters)	Plane	Containing Block	Camera
02/08/14	S609/SN094	600	704MD	26, 27	RCD024
02/09/14	S409/SN064	600	5726J	49	n/a
02/09/14	S609/SN094	600	704MD	27, 28	RCD024
02/10/14	S409/SN064	600	5726J	42, 43	n/a
02/14/14	S409/SN064	600	5726J	45	n/a
02/14/14	S609/SN094	600	704MD	28, 29	RCD024
02/16/14	S409/SN064	600	5726J	48	n/a
02/16/14	S609/SN094	600	704MD	29, 30	RCD024
02/17/14	S409/SN064	600	5726J	50, 52	PhaseOne
02/17/14	S609/SN094	600	704MD	31, 32	RCD069
02/18/14	S609/SN094	600	704MD	32, 33, 34	RCD069
02/19/14	S409/SN064	600	5726J	41	PhaseOne
02/19/14	S609/SN094	600	704MD	34, 35	RCD024
02/20/14	S409/SN064	600	5726J	40	PhaseOne
02/20/14	S609/SN094	600	704MD	35, 36	RCD024
02/22/14	S409/SN064	600	5726J	49, 50	PhaseOne
02/22/14	S609/SN094	600	704MD	37, 38	RCD024
02/23/14	S609/SN094	600	704MD	35, 36, 37, 38, 39	RCD024
02/24/14	S409/SN064	600	5726J	61, 62	PhaseOne
02/25/14	S409/SN064	600	5726J	60	PhaseOne
02/27/14	S409/SN064	600	5726J	59, 60	PhaseOne
02/27/14	S609/SN094	300	704MD	104	RCD024
02/27/14	S609/SN094	600	704MD	105	RCD024
02/28/14	S409/SN064	600	5726J	57	PhaseOne
02/28/14	S609/SN094	600	704MD	100, 101, 105	RCD024
03/01/14	S530/SN093	600	7320G	100	YES
03/01/14	S609/SN094	600	704MD	98	RCD024
03/02/14	S530/SN093	600	7320G	100	n/a
03/02/14	S609/SN094	600	704MD	100	RCD024
03/08/14	S409/SN064	600	5726J	55	PhaseOne



National Geodetic Survey

*Remote Sensing Division*

Flight Date	Sensors Used	Planned AGL (meters)	Plane	Containing Block	Camera
03/09/14	S409/SN064	600	5726J	54	PhaseOne
03/09/14	S609/SN094	600	704MD	99	n/a
03/10/14	S409/SN064	600	5726J	54	PhaseOne
03/10/14	S609/SN094	600	704MD	98	n/a
03/11/14	S409/SN064	600	5726J	53	PhaseOne
03/11/14	S609/SN094	600	704MD	98, 100	n/a
03/12/14	S409/SN064	600	5726J	53	PhaseOne
03/14/14	S409/SN064	600	5726J	53	PhaseOne
03/14/14	S609/SN094	600	704MD	100, 101	n/a
03/15/14	S609/SN094	600	704MD	100	RCD024
03/16/14	S409/SN064	600	5726J	112	PhaseOne
03/16/14	S609/SN094	600	704MD	100, 102	RCD024
03/20/14	S609/SN094	600	704MD	104	n/a
03/21/14	S409/SN064	600	5726J	111, 112	PhaseOne
03/21/14	S530/SN093	600	7320G	102	RCD
03/21/14	S609/SN094	600	704MD	103, 104	RCD024
03/22/14	S409/SN064	600	5726J	111	n/a
03/22/14	S530/SN093	600	7320G	106	RCD
03/22/14	S609/SN094	600	704MD	103, 107	RCD024
03/23/14	S409/SN064	600	5726J	111	n/a
03/24/14	S530/SN093	600	7320G	106, 108	n/a
03/24/14	S609/SN094	600	704MD	107, 108	SN024
03/27/14	S609/SN094	600	704MD	137, 138	n/a
03/31/14	S409/SN064	600	5726J	111	n/a
04/01/14	S409/SN064	600	5726J	110, 111	n/a
04/01/14	S530/SN093	600	7320G	136	n/a
04/01/14	S609/SN094	600	704MD	140	n/a
04/02/14	S409/SN064	600	5726J	110	n/a
04/02/14	S530/SN093	600	7320G	135	n/a
04/02/14	S609/SN094	600	704MD	139, 140	n/a

National Geodetic Survey

*Remote Sensing Division*

Flight Date	Sensors Used	Planned AGL (meters)	Plane	Containing Block	Camera
04/03/14	S409/SN064	600	5726J	109	n/a
04/03/14	S530/SN093	600	7320G	134	n/a
04/03/14	S609/SN094	600	704MD	127, 131, 132	n/a
04/05/14	S409/SN064	600	5726J	109	n/a
04/05/14	S609/SN094	600	704MD	130, 131	n/a
04/06/14	S409/SN064	600	5726J	109	n/a
04/06/14	S530/SN093	600	7320G	132, 133	DSS
04/06/14	S609/SN094	600	704MD	129, 130	n/a
04/07/14	S409/SN064	600	5726J	109	n/a
04/07/14	S609/SN094	300	704MD	138, 139	n/a
04/08/14	S530/SN093	300	7320G	132, 133, 134, 135	DSS
04/08/14	S609/SN094	300	704MD	139	n/a
04/09/14	S409/SN064	600	5726J	113	PhaseOne
04/09/14	S530/SN093	600	7320G	132	DSS
04/10/14	S409/SN064	600	5726J	113, 114	PhaseOne
04/10/14	S530/SN093	300	7320G	135, 136, 137	DSS
04/10/14	S530/SN093	600	7320G	132	n/a
04/11/14	S409/SN064	600	5726J	114, 115	PhaseOne
04/12/14	S409/SN064	600	5726J	115, 116	PhaseOne
04/12/14	S530/SN093	600	7320G	133	DSS
04/12/14	S609/SN094	600	704MD	126, 128	RCD024
04/13/14	S530/SN093	600	7320G	132	DSS
04/13/14	S609/SN094	600	704MD	125	n/a
04/16/14	S409/SN064	600	5726J	116, 117	PhaseOne
04/16/14	S530/SN093	600	7320G	133	DSS
04/17/14	S409/SN064	600	5726J	108	PhaseOne
04/17/14	S609/SN094	600	704MD	128, 129	RCD024
04/19/14	S609/SN094	600	704MD	121, 123	n/a
04/20/14	S609/SN094	600	704MD	124, 136	n/a
04/21/14	S609/SN094	600	704MD	123	RCD024

## National Geodetic Survey

*Remote Sensing Division*

Flight Date	Sensors Used	Planned AGL (meters)	Plane	Containing Block	Camera
04/21/14	S609/SN094	300	704MD	123, 125, 126	RCD024
04/28/14	S530/SN064	600	5726J	118	n/a
04/28/14	S609/SN094	600	704MD	122	n/a
04/29/14	S609/SN094	600	704MD	121, 122	n/a
05/01/14	S530/SN064	300	5726J	118	n/a
05/02/14	S530/SN064	600	5726J	108	n/a
05/02/14	S609/SN094	600	704MD	120, 121	n/a
05/03/14	S530/SN064	300	5726J	117, 118	n/a
05/03/14	S609/SN094	600	704MD	121	n/a
05/03/14	S609/SN094	300	704MD	119	n/a
05/04/14	S609/SN094	300	704MD	119, 120, 121	n/a
05/05/14	S530/SN064	300	5726J	117, 118	n/a
05/05/14	S609/SN094	300	704MD	121	n/a
05/06/14	S530/SN064	600	5726J	108	n/a
05/06/14	S530/SN064	300	5726J	108	n/a
05/07/14	S530/SN064	300	5726J	109, 117	n/a
05/07/14	S530/SN064	600	5726J	108	n/a
05/07/14	S609/SN094	600	704MD	51, 52	n/a
05/07/14	S609/SN094	300	704MD	49, 50, 51, 52, 53	n/a
05/08/14	S609/SN094	600	704MD	43, 44, 48, 50	n/a
05/08/14	S609/SN094	300	704MD	47, 48, 49	n/a
05/09/14	S609/SN094	300	704MD	41, 42, 43, 48, 49	n/a
05/09/14	S609/SN094	600	704MD	41	n/a
05/10/14	S609/SN094	600	704MD	38	n/a
05/10/14	S609/SN094	300	704MD	41, 44, 45, 46, 47	n/a
05/11/14	S530/SN064	300	5726J	111, 112	n/a
05/11/14	S609/SN094	300	704MD	33, 34, 35, 39, 40, 41	n/a
05/11/14	S609/SN094	600	704MD	30, 40	n/a

National Geodetic Survey

*Remote Sensing Division*

Flight Date	Sensors Used	Planned AGL (meters)	Plane	Containing Block	Camera
05/12/14	S530/SN064	300	5726J	109, 110, 111, 114, 115	n/a
05/12/14	S530/SN064	300	5726J	109	n/a
05/13/14	S609/SN094	300, 600	704MD	30, 31	n/a
05/14/14	S609/SN094	600	704MD	29	n/a
05/14/14	S609/SN094	300	704MD	27, 28, 29, 30	n/a
05/16/14	S609/SN094	300	704MD	15, 16	n/a
05/18/14	S609/SN094	300	704MD	21, 22, 25, 26, 27	RCD024
05/18/14	S609/SN094	600	704MD	26	RCD024
05/21/14	S530/SN064	600	5726J	67	PhaseOne
05/22/14	S530/SN064	600	5726J	66	n/a
05/22/14	S530/SN064	300	5726J	66, 67	n/a
05/22/14	S609/SN094	300	704MD	17, 18	n/a
05/23/14	S530/SN064	300	5726J	65, 66	n/a
05/23/14	S530/SN064	600	5726J	65	n/a
05/23/14	S609/SN094	300	704MD	1, 4, 5, 6, 7	n/a
05/24/15	S530/SN064	300	5726J	59, 61, 62	n/a
05/25/14	S530/SN064	300	5726J	59, 60, 61, 62	n/a
05/25/14	S609/SN094	300	704MD	22, 23, 24, 32	n/a
05/25/14	S530/SN064	600	5726J	60	n/a
05/26/14	S530/SN064	300	5726J	57, 58, 59, 60, 62	n/a
05/27/14	S530/SN064	300	5726J	63, 64, 65	n/a
05/30/14	S609/SN094	600	704MD	120, 121	n/a
05/31/14	S530/SN064	600	5726J	64	PhaseOne
05/31/14	S530/SN064	300	5726J	63	n/a
05/31/14	S609/SN094	600	704MD	119, 120	n/a
06/01/14	S530/SN064	300	5726J	63	n/a
06/01/14	S530/SN064	600	5726J	63, 64	n/a
06/01/14	S609/SN094	300	704MD	121, 122	n/a
06/02/14	S530/SN064	600	5726J	46, 53	PhaseOne

National Geodetic Survey

*Remote Sensing Division*

Flight Date	Sensors Used	Planned AGL (meters)	Plane	Containing Block	Camera
06/02/14	S530/SN064	300	5726J	54, 56, 57	PhaseOne
06/02/14	S609/SN094	300	704MD	140	n/a
06/03/14	S530/SN064	300	5726J	54, 55, 56	n/a
06/03/14	S530/SN064	600	5726J	43, 44, 45	n/a
06/03/14	S609/SN094	300	704MD	136, 137, 138, 139, 140	n/a
06/04/14	S530/SN064	300	5726J	68, 69	n/a
06/04/14	S609/SN094	300	704MD	126, 127	n/a
06/06/14	S609/SN094	300	704MD	115, 118	n/a
06/07/14	S530/SN064	300	5726J	74, 76, 77	PhaseOne
06/07/14	S609/SN094	300	704MD	112, 113, 114	n/a
06/08/14	S530/SN064	300	5726J	69, 70, 74, 75	PhaseOne
06/08/14	S530/SN064	300	5726J	69, 70	PhaseOne
06/08/14	S609/SN094	300	704MD	104, 107	n/a
06/09/14	S530/SN064	600	5726J	71	PhaseOne
06/09/14	S530/SN064	300	5726J	70, 71	PhaseOne
06/14/14	S530/SN064	300	5726J	72, 73, 74	n/a
06/15/14	S530/SN064	300	5726J	78, 79, 80, 81	n/a
06/15/14	S530/SN064	600	5726J	80	n/a
06/16/14	S530/SN064	300	5726J	80, 84	n/a
06/17/14	S609/SN094	300	704MD	101, 102	n/a
06/19/14	S530/SN064	600	5726J	80	n/a
06/20/14	S530/SN064	600	5726J	80	n/a
06/20/14	S609/SN094	300	704MD	98, 99, 101	n/a
06/21/14	S609/SN094	300	704MD	97, 98, 103	n/a
06/22/14	S609/SN094	300	704MD	93, 102	n/a
06/23/14	S530/SN064	600	5726J	80	n/a
06/23/14	S609/SN094	300	704MD	92, 94, 96, 97	n/a
06/24/14	S609/SN094	300	704MD	91, 95, 96	n/a
06/24/14	S609/SN094	600	704MD	94, 95	n/a

National Geodetic Survey

*Remote Sensing Division*

Flight Date	Sensors Used	Planned AGL (meters)	Plane	Containing Block	Camera
06/25/14	S609/SN094	300	704MD	90, 91	n/a
06/25/14	S609/SN094	300	704MD	90	n/a
06/27/14	S609/SN094	300	704MD	4, 8, 9, 10, 11	n/a
06/28/14	S530/SN064	300	5726J	81, 82, 83, 85	n/a
06/29/14	S530/SN064	300	5726J	86, 87, 88	n/a
06/29/14	S609/SN094	300	704MD	12, 13, 14	n/a
06/29/14	S609/SN094	600	704MD	12, 13, 14	n/a
06/30/14	S530/SN064	300	5726J	88, 89	n/a
06/30/14	S609/SN094	600	704MD	21	n/a
07/01/14	S530/SN064	600	5726J	80	PhaseOne
07/01/14	S530/SN064	300	5726J	80, 81	PhaseOne
07/01/14	S609/SN094	600	704MD	30, 38, 39, 40, 43, 45, 46	n/a
07/03/14	S530/SN064	300	5726J	80	n/a
07/06/14	S530/SN064	600	5726J	75, 76	PhaseOne
07/07/14	S530/SN064	300	5726J	65	n/a
07/08/14	S530/SN064	600	5726J	75	PhaseOne
07/08/14	S530/SN064	300	5726J	80	PhaseOne
07/09/14	S530/SN064	300	5726J	80	PhaseOne
07/11/14	S530/SN064	600	5726J	80	PhaseOne
07/13/14	S609/SN094	600	704MD	25, 27	RCD069
07/14/14	S530/SN064	600	5726J	80	PhaseOne
07/14/14	S609/SN094	600	704MD	40	RCD069
07/16/14	S530/SN064	300	5726J	80	PhaseOne
07/17/14	S530/SN064	300	5726J	80	n/a
07/17/14	S530/SN064	300	5726J	80	n/a
07/20/14	S530/SN064	300	5726J	27	PhaseOne
07/21/14	S530/SN064	600	5726J	23	PhaseOne
07/25/14	S530/SN064	600	5726J	33	PhaseOne
07/26/14	S530/SN064	600	5726J	36, 37	PhaseOne



### 4.3. Data Processing Methods & Procedures

Dewberry performed all final QAQC of the lidar data and imagery, including horizontal and vertical accuracy testing. Dewberry surveyors collected the independent checkpoints used in the final accuracy testing. And Dewberry created all final topobathy DEMs and associated DEM products.

RSD performed further QC of the lidar data and derived the initial shoreline files from the delivered topobathy lidar point cloud and the digital imagery. The shoreline files were then sent back to Dewberry for clean-up and attribution.

#### 4.3.1. Field Processing

Because of the complexity of the project, some of the lidar processing evolved over the course of the project as we refined our processes and found the most efficient methods.

The Riegl sensors used for the Supplemental Sandy project had the detector set to very sensitive settings in an effort to acquire as much bathymetric data as possible. However, the sensitivity resulted in a great deal of noise. The additional noise added time to the automated classification algorithms because the software had to sift through additional points. The additional noise added to manual classification time because not only were there more points to look at, but quite a bit of the noise was close to valid bathymetric points so it took additional time to differentiate between bathy bottom and noise. Additionally, the sensitivity settings resulted in an incredibly dense water column. There were so many points that the lidar had to be tiled to 500 m x 500 m tiles instead of 1000 m x 1000 m tiles because software could not handle the number of points that would be within the larger tiles.

Throughout the course of the project several types of features were identified, including oyster beds, very small barrier islands, and breakwater features. If these were new features like oyster beds and they were not on the chart the Marine Chart Division was notified and geographic coordinates were submitted with images of the area so MCD could look into the permitting aspect and coordinate with the appropriate authorities.



### 4.3.2. Workflow Overview

Figure 6 below outlines the general workflow of the contractors for this project.

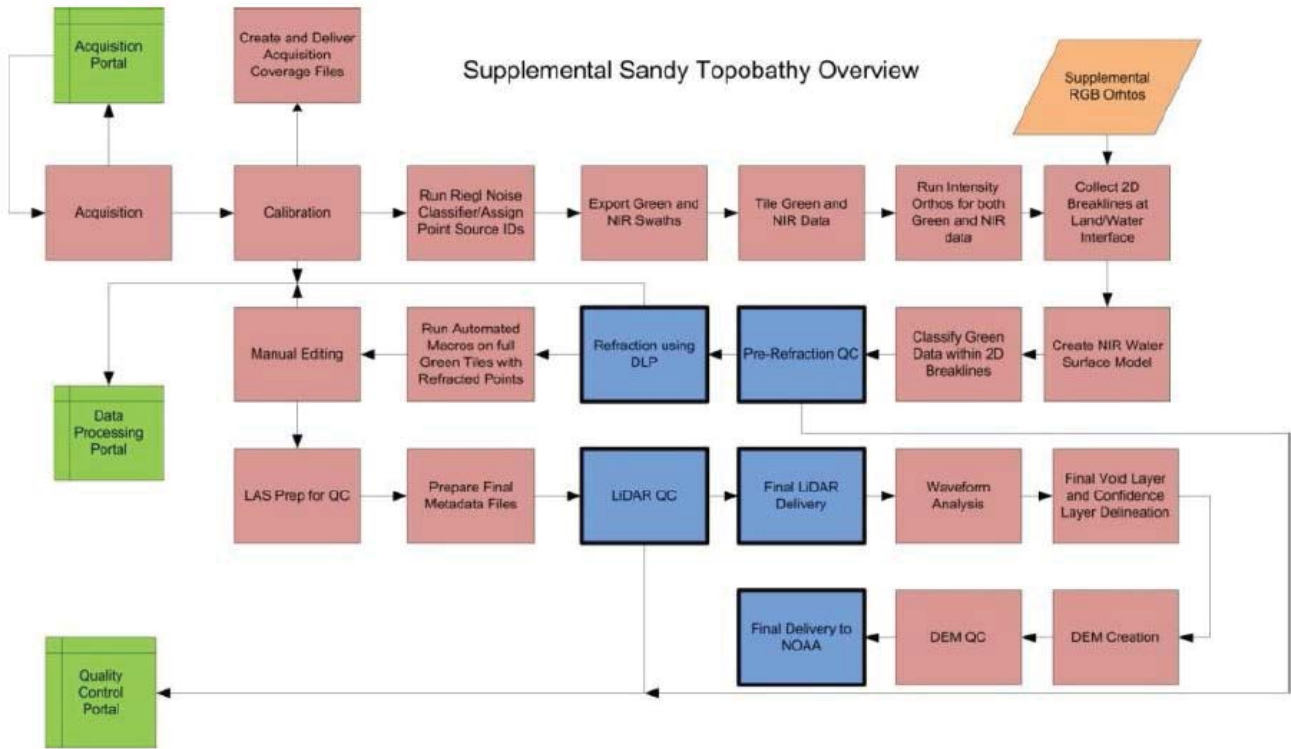


Figure 6. SSP Topobathy Overview

Figure 7 outlines the general workflow of RSD.

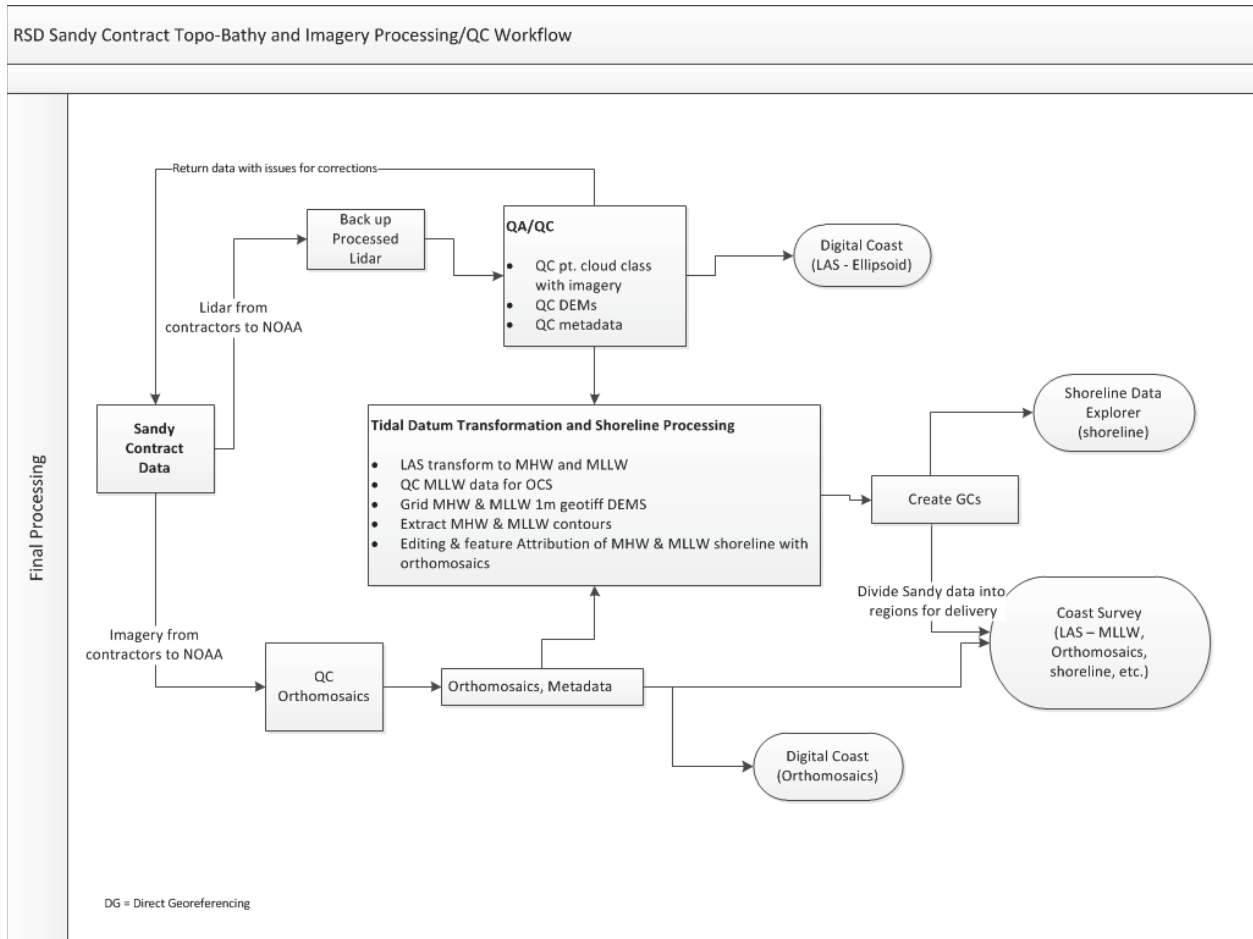


Figure 7. RSD Sandy Contract Topo-Bathy and Imagery Processing Workflow

### 4.3.3. Trajectory Processing

Solutions for best estimates of trajectory were processed using Applanix POSpac 6.2 SP2. This process utilizes the GPS (recorded at 2Hz) and IMU (200Hz) data recorded onboard the aircraft, static base stations established over control monuments, and differential GPS/GLONASS processing to calculate the most precise position of the aircraft.

#### 4.3.4. Lidar Processing

After acquisition, the contractors calibrated the raw data. The calibration included calibration to ground control as well as swath to swath calibration within a mission and between missions (including MLLW to HW) and calibration between the NIR and green swaths. Co-registration between the NIR and green was vital as the NIR data was used to produce the water surface models for refraction. Additionally, NIR data served as a “back-up” in case there are any voids or sensor anomalies/issues that cannot be filled or corrected in the green topographic data.

The initial calibration of the green data (control and line to line) was performed in RiProcess. Any processing specific to RiProcess, such as the noise classifier, was performed prior to exporting the data from the RiProcess project.

Sensor noise was classified within the RiProcess software before data was exported to LAS format. For efficiency, TerraScan was used to set all point source ID’s in the Sandy project vice using RiProcess. Once the green swath data was exported to LAS format, the green swaths were compared and calibrated with the NIR swaths. Due to the size of the swaths, the data was tiled and then calibration was performed on the tiles. In addition to calibrating between adjacent lines within a mission, mission to mission calibration was also performed. This included calibration between production blocks that were been acquired at different time periods.

#### **Breaklines**

Breaklines representing the land/water interface were also created and were used to determine which LAS points would go through the refraction correction tool. These breaklines were 2D polygons. Automated methods of breakline collection were used where possible and were manually reviewed and edited/adjusted where necessary by the primary contractor and RSD. All features, regardless of size, identified as water through automated routines and verified as correct remain in the dataset.

As part of the breakline processing and review, ensure really tiny, extraneous ‘donut holes’ were cleaned out of the breaklines so that it did not cause classification issues in the lidar. Dewberry used ArcGIS tools to remove these from the dataset.

#### **Refraction**

The Green and NIR data was classified using the 2D breaklines. Green data falling within the 2D breaklines was refracted. NIR data falling within the breaklines was used to create some of the water surface models that were an input for the refraction tool. NIR data was used in inland areas where there are no water surface points or very few water surface points in the green data. Water surface models was created from the green data along the shoreline where waves and varying water surface heights can impact the refraction correction. Where bays and inlets empty into the ocean, the data was logically split near the mouth so that data inland from that point was refracted using NIR water surface models and data seaward from that point was refracted using green water surface models.

**Water Surface Model Creation**

Only one water surface model was used by the refraction tool. NIR water surface points were combined with Green water surface points in one IMG file. NIR water surface points were used inland where NIR and Green water surface elevations were consistent and where the density of green water surface points were sometimes sparse and inconsistent.

Green water surface points were used along the shoreline and outer coast where sufficient green water surface points exist and where wave action existed, creating disparities between NIR and green water surface elevations.

The NIR and green water points were combined into one single IMG file using Global Mapper software. The combined water surface model was in IMG format with 1 meter grid cell size. To ensure full coverage of the extents of each input LAS files, the water surface models were created to the extent of the 500m x 500m tile.

**Pre-refraction QC**

The pre-refraction QC primarily verifies coverage and calibration or relative accuracy. It was performed prior to refraction in case any corrections need to be applied so that corrections are done prior to refracting any data which would require re-refracting the data. In addition to verifying coverage and calibration, the pre-refraction QC also includes reviewing breaklines and water surface models.

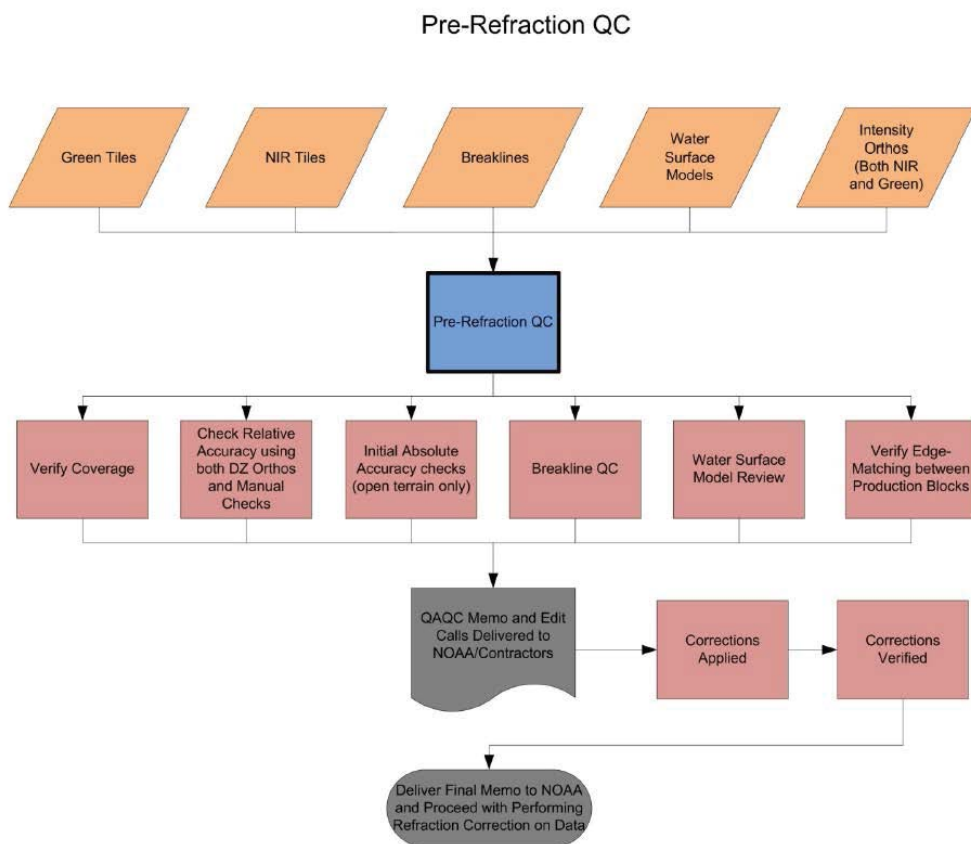


Figure 8. Pre-Refraction QC workflow

### Verify Extents

The extents for each block of data was created to verify full coverage. Point classifications were reviewed on green data to ensure data is classified properly (incorrect green data point classifications would impact the refraction tool results). The data extents were reviewed for both the Green and NIR data.

### Relative Accuracy QC

The relative accuracy between green data (swath to swath and MLLW to HW) as well as the relative accuracy between green and NIR data was verified using DZ orthos and manual checks.

### Refraction

Once data has passed all pre-refraction QC, the data was ready for the refraction tool. The refraction tool used the water surface model and mission Smoothed Best Estimate of Trajectory (SBET) to perform refraction (correcting for time/distance and horizontal movement of LiDAR points in water) on all green LiDAR points classified as water column (water column classification based on breaklines). The refraction tool created a new output and did not modify the input tiles. The general refraction workflow is shown below:

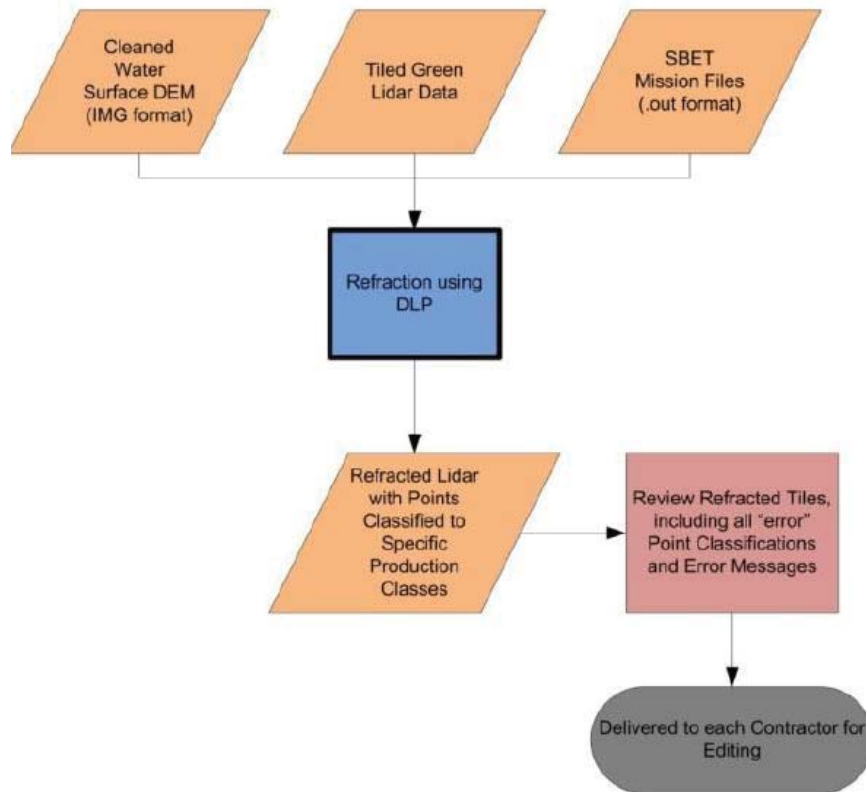


Figure 9. Refraction correction process workflow

#### 4.3.5. Lidar Editing

For each block in the SSP, the workflow steps for editing topobathy lidar data are provided below:

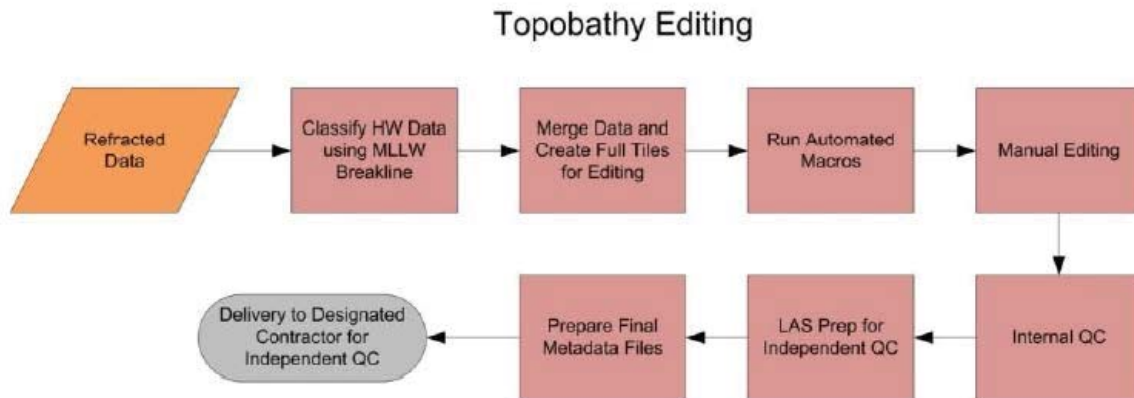


Figure 10. Contractor workflow for topobathy editing

During automated macros (to remove air and low points, remove noise, etc.) and manual editing (remove remaining bathy noise or misclassified points, etc.), points are never removed but are rather classified to another class layer in Terrascan.

#### 4.3.6. Product Creation

Once production and all edits are complete, the LAS files was finalized and the final classification schema was delivered per RSD's guidance:

Table 10. Final LAS Deliverable to RSD from Sandy Contractors

<b>LiDAR Classification – Final Deliverables</b>	
<b>Class</b>	<b>Description</b>
Class 1	Unclassified
Class 2	Ground (Topo)
Class 7	Topo Noise (low or high)
Class 18	Refracted High Water (HW) points landward of the MLLW land/water interface breakline
Class 22	Bathy Noise (Unrefracted green points higher than the NIR water surface)
Class 23	Sensor Noise (all sensor noise-as classified by the sensor software RiProcess-over land, only unrefracted sensor noise points over water)
Class 24	Sensor noise Refracted
Class 25	Water Column (No Bottom Found)
Class 26	Bathy Bottom (Submerged Topography)
Class 27	Water Surface
Class 30	International Hydrographic Organization (IHO) S-57 object, not otherwise specified
Class 31	Temporal Bathy Bottom (Bathy Bottom points in areas of temporal change not used in the final bathy bottom classification)
Class 139	Points flagged with the withheld bit will show as classification 139 in TerraScan

RSD split up each of these files into their own separate files for use by HSD. Only classification LAS files: 1, 2, 25, 26, 27, 29 and 30 were will be submitted to HSD per their request.

LAS files containing all the data were loaded into Global Mapper to create a grid for each SSP block. Once the grid was created in Global Mapper and exported, ESRI ArcGIS software was used to convert all NoData pixels to polygons and output a raster.

A confidence layer was created for each production block and reports the standard deviation of all ground and submerged topography points within each one meter grid cell. The confidence layer has the same extents as the final topobathy DEMs so that the pixels align, showing the confidence of each topobathy DEM grid cell.

A density layer was also created to identify the number of ground and/or submerged topography points located in each one meter grid cell.

#### 4.3.7. Imagery Processing

The RGB imagery acquired was used to generate an orthorectified mosaic. This mosaic was used to assist in data editing and is provided as a final product.

#### 4.3.8. Additional Quality Checks

The primary contractor, Dewberry, ensured independent quality control on the subcontractors' data and often cleaned the data internally staff to improve efficiency. In the beginning, NOAA and Dewberry found some inconsistency issues that had to be addressed and in some blocks it resulted in numerous rounds of corrections. The training and learning curve from SSP will benefit other future RSD topobathy projects and improve efficiency.

DZ ortho quality checks were performed to ensure there are no relative accuracy or elevation discrepancies in the final ground/submerged topography surface model. High DZ values can typically be seen along slopes or vegetated areas where higher and lower elevation points are within one pixel cell due to terrain change/height of vegetation.

In addition to using DZ orthos, manual checks will be performed on a sample of tiles.

### 4.4. Corrections to measurements

Corrections to lidar data which affect the overall resultant depth include system offsets, calibration values, aircraft motion corrections, and environmental parameters used during processing. In addition to this, datum transformations have an effect on the overall depth accuracy.

#### 4.4.1. System Offsets and Lidar Calibrations

Lidar data calibration occurred at the start and end of the SSP. System offsets within the Riegl lidar system are constant and will not change until the sensor is uninstalled or moved. But the offset from the GNSS antenna to the center of the IMU was calculated each time the system is installed or the GNSS moved or changed.

#### 4.4.2. Motion Corrections

Solutions for best estimates of trajectory were processed using Applanix POSPac 6.2 SP2. This process utilizes the GPS (recorded at 2Hz) and IMU (200Hz) data recorded onboard the aircraft, static base stations established over control monuments, and differential GPS/GLONASS processing to calculate the most precise position of the aircraft.



#### 4.4.3. Environmental Parameters/Processing Settings

As stated in section 4.2.1., weather was the biggest problem encountered and an additional classification was added to the final classification schema; class 31-temporal bathy bottom.

Data along the shoreline or land/water interface could be collected multiple times-at mean lower low water level (MLLW) and higher water levels (HW). MLLW has specific requirements whereas HW in this document represents everything not collected at MLLW. RSD advised the contractors that collecting data during times where there was good water clarity should take precedence over tidal requirements. HW and MLLW data were combined into 500m x 500m tiles. The combination of MLLW and HW data resulted in areas of temporal change due to temporal variation between the different flight lines.

#### 4.4.4. Vertical Datum Conversions

VDatum 3.4 was used to convert data from NAD83 (2011) elevations to Mean Lower Low Water (MLLW), which made use of GEOID12A. Uncertainties associated with both the source data and each transformation used during the conversion within VDatum is computed. The Cumulative uncertainty was calculated as follows for the different regions within the SSP:

Region	Cumulative Uncertainty (NAD83 to MLLW)
<b>Georgia/South Carolina</b>	14.68
<b>North Carolina Coastal Shelf</b>	8.56
North Carolina Inland waterways and sounds	8.15
<b>Virginia/Maryland - Chesapeake Bay</b>	7.70
Virginia/Maryland/Delaware - Coastal Embayments	7.34
Delaware - Delaware Bay	9.47
<b>Virginia/Maryland/Delaware- Mid Atlantic Bight Shelf</b>	7.31
New Jersey - Coastal embayments	7.70
New Jersey/New York/Connecticut - Norther New Jersey, NY Harbor, western Long Island Sound	7.92
New York - The Great South Bay	10.49
New York/Conneticut/Rhode Island - Outer NY Bight, eastern Long Island Sound, Block Island Sound	8.27

## 5.0 Uncertainty

### Lidar Positional Accuracy

The vertical accuracy of the lidar was tested with 261 checkpoints collected in five land cover categories:

- Brush Lands and Low Trees
- Tall Weeds/Crops
- Urban/Open Terrain
- Fully Forested
- Submerged Topography

Only checkpoints photo-identifiable in the lidar intensity imagery could be used to test the horizontal accuracy of the lidar so only nine (9) checkpoints were used for horizontal accuracy testing.

### Lidar Vertical Accuracy

Project specifications required Open Terrain/Urban to meet 24.5 cm at the 95% confidence level based on  $RMSE_z (12.5 \text{ cm}) \times 1.9600$ . Submerged topography was required to meet 49 cm at the 95% confidence level based on  $RMSE_z (25 \text{ cm}) \times 1.9600$ . Consolidated Vertical Accuracy (CVA) was required to meet 36 cm based on the 95th percentile and Supplemental Vertical Accuracy (SVA) was targeted at 36 cm based on the 95th percentile. Final vertical accuracy of the lidar and all associated statistics are shown below; the lidar data pass vertical accuracy requirements.

*Table 11. Open Terrain must meet 24.5 cm Accuracy while Submerged Topography must meet 49cm Accuracy. CVA and SVA must meet 36 cm based on the 95th percentile*

Land Cover Category	# of Points	ACCURACY <sub>z</sub> (RMSE <sub>z</sub> x 1.9600) m	CVA – Consolidated Vertical Accuracy (95th Percentile) m	SVA – Supplemental Vertical Accuracy (95th Percentile) m
Consolidated	261		0.226	
Brush Lands and Trees	63			0.240
Tall Weeds/Crops	68			0.227
Urban/Open Terrain	62	0.153		
Forested	68			0.176
Submerged Topography	52	0.323		

Table 12.  $RMSE_z$  for open terrain checkpoints must meet 12.5 cm while  $RMSE_z$  for submerged topography points must meet 25 cm.

Land Cover Category	# of Points	$RMSE_z$ (m)	Mean (m)	Median (m)	Skew	Std Dev (m)	Kurtosis	Min (m)	Max (m)
Consolidated	261		0.059	0.050	-2.078	0.101	25.073	-0.843	0.435
Brush Lands and Trees	63		0.085	0.071	1.329	0.089	2.611	-0.055	0.421
Tall Weeds/Crops	68		0.097	0.096	0.873	0.084	2.834	-0.109	0.435
Urban/Open Terrain	62	0.078	0.019	0.023	2.023	0.076	11.163	-0.158	0.414
Forested	68		0.033	0.040	-5.161	0.126	35.921	-0.843	0.237
Submerged Topography	52	0.165	0.051	0.027	2.378	0.158	9.682	-0.227	0.809

There were 13 outliers. These 5% outliers had lidar-checkpoint elevation differences ranging from -0.843 m to +0.435 m.

### Lidar Horizontal Accuracy

Horizontal accuracy cannot always be tested on elevation data as horizontal accuracy testing requires well-defined points. Dewberry reviewed all urban/open terrain checkpoints to determine if any of the checkpoint locations could be identified on the lidar intensity imagery. As only nine (9) checkpoints were photo-identifiable, the results are not statistically significant, but are shown in the table below. Project specifications required calibration procedures that would result in lidar data produced to meet 1 meter  $RMSE_r$ , which equates to 1.7308 m at the 95% confidence level based on  $RMSE_r \times 1.7308$ . Based on the limited number of photo-identifiable checkpoints, the lidar data passes horizontal accuracy requirements.

Table 13. Horizontal accuracy of the lidar was calculated using survey checkpoints photo-identifiable in the intensity imagery. Horizontal accuracy at the 95% confidence level,  $ACCURACY_r$ , is required to meet 1.7308 meters based on  $RMSE_r \times 1.7308$ .

# of Points	$RMSE_x$ (Spec=0.707 m)	$RMSE_y$ (Spec=0.707 m)	$RMSE_r$ (Spec=1 m)	$ACCURACY_r$ ( $RMSE_r \times 1.7308$ ) Spec=1.7308 m
9	0.354	0.362	0.507	0.877

### DEM Vertical Accuracy

The same checkpoints used to test the vertical accuracy of the lidar data were also used to test the vertical accuracy of the DEM data to ensure all products, even those derived from the source lidar data, pass vertical accuracy specifications. The DEMs are created using controlled methods to limit the amount of error introduced during DEM production but differences between the source LiDAR and final DEMs do exist due to interpolation differences. DEMs are created by averaging several LiDAR points

Remote Sensing Division

within each pixel which may result in slightly different elevation values at a given location when compared to the source LAS, which does not average several LiDAR points together but may interpolate (linearly) between two or three points to derive an elevation value used in vertical accuracy testing. In DEM vertical accuracy testing, the value of the pixel containing each survey checkpoint is extracted and compared to the surveyed elevations. Final vertical accuracy of the DEMs and all associated statistics are shown below; the DEM data pass vertical accuracy requirements.

Table 14. Open Terrain must meet 24.5 cm Accuracy<sub>z</sub> while Submerged Topography must meet 49 cm Accuracy<sub>z</sub>. CVA and SVA must meet 36 cm based on the 95th percentile.

Land Cover Category	# of Points	ACCURACY <sub>z</sub> (RMSE <sub>z</sub> x 1.9600) Spec=0.245 m for Open Terrain and 0.49 m for Submerged Topography	CVA – Consolidated Vertical Accuracy (95th Percentile) Spec=0.36 m	SVA – Supplemental Vertical Accuracy (95th Percentile) Target=0.36 m
Consolidated	261		0.215	
Brush Lands and Trees	63			0.254
Tall Weeds and Crops	68			0.240
Urban/Open Terrain	62	0.112		
Forested and Fully Grown	68			0.142
Submerged Topography	52	0.331		

Table 15. RMSE<sub>z</sub> for open terrain checkpoints must meet 12.5 cm while RMSE<sub>z</sub> for Submerged Topography points must meet 25 cm.

100 % of Totals	# of Points	RMSE <sub>z</sub> (m) Open Terrain Spec=0.125 m Submerged Topography Spec = 0.25 m	Mean (m)	Media n (m)	Skew	Std Dev (m)	Kurtosis	Min (m)	Max (m)
Consolidated	261		0.066	0.055	1.224	0.084	3.780	-0.162	0.487
Brush Lands and Trees	63		0.092	0.069	1.556	0.098	4.254	-0.077	0.487
Tall Weeds and Crops	68		0.104	0.093	0.761	0.088	1.698	-0.101	0.423
Urban/Open Terrain	62	0.057	0.015	0.026	-0.504	0.055	0.798	-0.162	0.126
Forested and Fully Grown	68		0.051	0.042	0.615	0.057	0.632	-	0.218
Submerged Topography	52	0.169	0.058	0.038	2.047	0.160	7.591	-0.233	0.785

There were 13 outliers. These 5% outliers had lidar-checkpoint elevation differences ranging from +0.218 m to +0.487 m.

**Ortho-Mosaic horizontal accuracy**

The final horizontal accuracy of the ortho-mosaics was calculated with 46 photo-identifiable checkpoints. The ortho-mosaics were required to meet 1.7308 meters at the 95% confidence level based on  $RMSE_r \times 1.7308$ . The statistics are shown in the table below; the ortho-mosaics meet all horizontal accuracy specifications.

*Table 16. The Supplemental Sandy ortho-imagery meets horizontal accuracy requirements per the SSP SOW.*

# of Points	$RMSE_x$ (Spec=0.707 m)	$RMSE_y$ (Spec=0.707 m)	$RMSE_r$ (Spec=1 m)	ACCURACY <sub>r</sub> ( $RMSE_r \times 1.7308$ ) Spec=1.7308 m
46	0.227	0.208	0.307	0.532

**6.0 Vertical and Horizontal Control**

A description of the vertical and horizontal control requirements can be found in the SOW for Shoreline Mapping in support of Public Law No: 113-002, Disaster Relief Appropriations Act 2013.

The horizontal datum for this project is North NAD 83 (2011)

The projection used for this project is NAD83 UTM Zone 18 North

Ground survey information is explained in section 4.1.1.3 and GPS derived heights were transformed from the reference ellipsoid to the chart datum (MLLW) as explained in section 4.4.4.

**7.0 Results and Recommendations**

Recommend further investigation for any charted feature not found in fully covered bathymetric lidar data areas.

## Letter of Approval

This report and the accompanying data are respectfully submitted.

Contract operations contributing to the accomplishment of survey W00303 (NY-1409) were conducted under my supervision with frequent checks of progress and adequacy as well as quality assurance of the outputs. This report and associated data have been closely reviewed and are considered complete and adequate as per the LIDAR and Digital Cameral Imagery Requirements Scope of Work for Shoreline Mapping in Support of Public Law No: 113-002, Disaster Relief Appropriations Act 2013 and where possible the NOS Hydrographic Surveys Specifications and Deliverables (2014).

**ASLAKSEN.MICHAEL.L.JR.1090880230**  
**L.L.JR.1090880230**

Digitally signed by  
ASLAKSEN.MICHAEL.L.JR.1090880230  
DN: c=US, o=U.S. Government, ou=DoD, ou=PKI,  
ou=OTHER, cn=ASLAKSEN.MICHAEL.L.JR.1090880230  
Date: 2016.02.09 16:27:02 -05'00'

---

Michael L. Aslaksen, Jr.

Chief, Remote Sensing Division

NOAA's National Geodetic Survey